

Review report to “Flocculation processes and sedimentation of fine sediments in the open annular flume - Experiment and numerical modeling” by Klassen et al, ESURF-2013-19.

I have read the manuscript with great interest and I have appreciated it because it tackles a topic I am particularly interested in. In general, English should be improved because it is not written clearly in many instances. Not all figures are necessary; for example, Figure 1 can be removed and probably also Figure 2. Figure 12, does not help much in interpreting the results. There are a number of minor issues that the authors should address, and are marked in the marked copy. Some major issues must be addressed before the manuscript can be considered for publication, and are discussed in detail below.

Major comments

The authors should rephrase the abstract because it is not straight to the point and is a bit loose. Besides, the finding they put forth in the abstract is that “the settling behavior was very sensitive to variations in the fractal dimension”. This result is not new; it is very well understood since earlier works by Han Winterwerp, Fede Maggi and Paul Hill. I wonder if this is enough a finding for a publication. I suggest the authors to truly revisit their work and see if there is any additional key quantitative result that should be stated in the abstract to make their work more appealing.

Page 3, L1, yield strength is not the only physical characteristic that determines the outcome of a collision but other effects are equally, if not more, important such as the double layer interaction.

Page 4, L1 to 4 is not clear while this is an essential part of the understanding and replicability of the results presented here. Please, explain well what the boundary conditions are and what criteria have driven the design of your set-up.

Page 4, L11. I was a bit concerned to read that greatest errors were found in the way the model describes the kinetic energy because flocculation (both aggregation and break) is predominantly governed by turbulence shear. If a big bias is present at that level, then I may infer that all flocculation processes implemented in SSIIM are somehow biased. Could the author please carefully revise the manuscript in this aspect and possibly improve it?

Page 4, L 18. If there were several experiments runs in the annular flume, why only one set of experiments was used in this manuscript? Use of one data set allows for parameter estimation only, that is, you cannot validate the parameters and the mathematical framework on an independent data set. This is a serious issue that will come up again later in my comments.

Page 4, L 29. The turbidity meter measures the turbidity but not the concentration. This is an important aspect just because the authors are dealing with cohesive sediment. If they were using silt it would be ok, but with kaolinite, turbidity decreases as flocculation proceeds even if the concentration is constant. The authors should be aware of the fact that this is introducing a systematic error in their measurements or in the way they use the measurements for the calibration of their model. In any case, they should discuss this in the manuscript.

Page 5, L7 to 12. I would suggest to add an appendix where the author could add a brief description of the image post-processing algorithms.

Page 5, L27. That one is the turbidity, not the concentration. Have you calibrated the turbidity meter against known concentrations?

Page 5, L 30. The authors have run 70 hours of experiments, so why do compare the model over the first 5 hours only? Even if the calculation time is long (say in the order of day) I would suggest to invest that time to achieve a deeper analytical introspection of how the model works and how to improve it should things go not that well.

Page 6, L4 to 25. Overall, Figure 5 shows that the turbidity decreases (perhaps an evidence that flocculation takes place) while Figure 6 shows that d50 and d90 decrease. Although the interpretation put forth is ok in that concern with the increasing deposition, I have doubts to clearly distinguish any sign of flocculation occurring in those experiments. Even if the authors suggest that flocculation occurs because of the first peak in d50 and d90 in Figure 6 and show the floc images in Figure 7, I have to be frank that I do not see any real difference, and I can even imagine that the peak in Figure 6 could be due to some type of interference or experimental noise. What I mean is that the interpretation put forth is based on a very weak signal. I have no real suggestion to the authors to cope with this, but the overall impression is that results do not show clear evidence of flocculation processes.

Page 7, L 25. That is ok, but it is a very strong assumption. Have you done some verification of it? Perhaps calculating the double layer repulsive and attractive forces, and see where the force balance supports your statement?

Page 8, L13, What do the authors mean with real fractal structures having a smallest and largest dimension? Please clarify.

Page 11, L1 to 17. I am also in this case a bit confused. A comparison with the Winterwerp and Stokes settling velocity is fine. However, the Winterwerp equation in the form reported by the authors is just proportional to the Stokes law with the exception of the shape prefactor ratio α/β . Because the authors use spherical flocs (Page 11, L 27), then $\alpha/\beta = 1$, and the Winterwerp equation becomes identical to the Stokes equation. I wonder what the authors have compared in their results. This aspect is serious enough to necessarily be corrected before considering this manuscript for publication. In any case, I would recommend the authors to review recent works on the settling velocity of fractal flocs, where they may find newer and better frameworks.

Page 11, L 27. See assumption of spherical particles and implication as mentioned above.

Page 13, L 11. This point goes back to the comment arose earlier about the 5 h time simulation as compared to the 70 hour experiment. Figure 13 does not show all the story. For $n_f = 1.4$, experimental data and model suggest that they depart largely soon after 5 h cut off. This aspect is critical and does not truly convince me that the matching is good enough unless the authors show experiments and model results for $t > 5h$ as well (say 10 hours up to maybe 20 hours). This is still computationally doable as compared to 70 hours – I believe.

Page 13, L 29. In commenting Figure 14, the authors should note that experimental d50 and modeled d50 are anticorrelated, which is not a good sign of matching between experiments and simulations. I

am not sure that the model is working well as I see these figures (13 and 14 in particular). Same as before, the authors should extend the comparison time to 10 or 20 hours also for d50.

Page 14, L 27, what values of alpha and beta have the authors used? My understanding is that they assumed $\alpha=\beta=1$; if so, the statement at this line would be a contradiction, because the settling velocity used in the model would be the Stokes velocity and not the Winterwerp velocity.

Section 4.4. This section collects all critical aspects I have commented about the previous sections and brings them together. I believe that this section should be revised largely according to any revisions brought about to address earlier critical points.

Conclusions points to some minor (but not too minor) aspects that are a reflection of the criticalities discussed above in my comments. I have marked several of them in the marked manuscript, but I recommend the authors to thoroughly revise their conclusions after a deeper investigation of model as compared to experiments.

Overall, I miss a discussion section, where critical points such as systematic errors, experimental errors, assumptions and others hypotheses and results are discussed against the existing knowledge, data, and modeling frameworks.

Minor comments

I have implemented several comments and pointed to unclear writing in the marked copy of the manuscript appended here. Some are very minor, some other address to major concerns.

I believe that the manuscript may be of interest to Earth Surface Dynamics, but I think that major revisions must be implemented before consideration for publication. I think that if some criticalities cannot be correct at this stage, the manuscript could be withdrawn and resubmitted at a later stage to make sure that the material is at the highest scientific level and appealing to the wider sediment community.

Kind regards

1 Flocculation processes and sedimentation of fine sediments in 2 the open annular flume - Experiment and numerical modeling

3

4 I. Klassen¹, G. Hillebrand², N. R. B. Olsen³, S. Vollmer², B. Lehmann⁴ and F.
5 Nestmann¹

6 [1]{Institute for Water and River Basin Management, Karlsruhe Institute of Technology, Germany}

7 [2]{Federal Institute of Hydrology, Koblenz, Germany}

8 [3]{Department of Hydraulic and Environmental Engineering, Norwegian University of Science
9 and Technology, Trondheim, Norway}

10 [4]{Institute for Hydraulic Engineering and Water Management, Technical University Darmstadt,
11 Germany}

12 Correspondence to: I. Klassen (irina.klassen@kit.edu)

13

14 Abstract

15 The prediction of cohesive sediment transport requires numerical models which include the
16 dominant physico-chemical processes of fine sediments. Mainly in terms of simulating small scale
17 processes, flocculation of fine particles plays an important role since aggregation processes affect
18 the transport and settling of fine-grained particles. Flocculation algorithms used in numerical
19 models are based on and calibrated using experimental data. A good agreement between the results
20 of the simulation and the measurements is a prerequisite for further applications of the transport
21 functions. *???*

22 In this work, the sediment transport model (SSIIM) was extended by implementing a physics-based
23 aggregation process model based on McAnally (1999). SSIIM solves the Navier-Stokes ~~Equations~~
24 in a three-dimensional, non-orthogonal grid using the k-ε turbulence model. ~~The program~~ calculates
25 the suspended load with the convection-diffusion equation for the sediment concentration. *SSIIM*

26 Experimental data from studies in annular flumes (Klassen 2009, Hillebrand 2008) is used to test
27 the flocculation algorithm. Annular flumes are commonly used as a test rig for laboratory studies on
28 cohesive sediments since the flocculation processes are not interfered with by pumps etc. We use
29 the experiments to model measured floc sizes, affected by aggregation processes, as well as the
30 sediment concentration *it* of the experiment. Within the simulation of the settling behavior, we use *?*

Algorithms describing flocculation

that

Not clear

against

Not clear why it should

this is not a new result....

1 different formulas for calculating the settling velocity (Stokes 1850 vs. Winterwerp 1998) and
2 include the fractal dimension to take into account the structure of flocs.

3 The aim of the numerical calculations is to ^{validate} evaluate the flocculation algorithm by comparison with
4 the experimental data. The results from these studies have shown, that the flocculation process and
5 the settling behaviour are very sensitive to variations in the fractal dimension. We get the best
6 agreement with measured data by adopting a characteristic fractal dimension n_{fc} to 1.4. Insufficient
7 results were obtained when neglecting flocculation processes and using Stokes settling velocity
8 equation, as it is often done in numerical models ^{that} which do not include a flocculation algorithm.

equal?

9 These numerical studies will be used for further applications of the transport functions to the SSIIM
10 model of reservoirs of the Upper Rhine River, Germany.

-----?

12 **1 INTRODUCTION**

Why end here?

13 Suspended sediment dynamics is an important and complex field within sediment transport. Several
14 issues may illustrate the relevance of fine, cohesive sediments: high sediment loads lead to an
15 impairment of the flora and fauna, colmation due to fine sediments can cause a loss of habitats, and
16 in areas with low flow velocities (e.g. at ports, in groyne fields and at barrages) sedimentation of
17 fine-grained sediments takes place and involve cost-intensive maintenance dredging (Brunke 1999,
18 Winterwerp and van Kesteren 2004, Yang 1996). In addition, in case of contaminations, cohesive
19 sediments may pose even more serious ecological and economic problems. Numerical modeling of
20 the interaction between cohesive sediments, particle-bound contaminants and the water flow
21 represents a major challenge in morphodynamics and sediment engineering.

22 The physical characteristics and the behavior of fine-grained sediments, that Mehta and McAnally
23 (2007), for instance, defines as grains that are less than 63 μ m in size, are affected by numerous
24 parameters (see Fig. 1): physico-chemical factors (e.g. particle properties, particle concentration,
25 salt content, pH-value, temperature), biological (e.g. organic matter,) and flow-dependent factors
26 (e.g. flow velocity, turbulence intensity). The sorption and adsorption processes of particle-bound
27 contaminants on the other hand are impacted by many factors as well: e.g. organic matter content in
28 the suspended matter, water chemistry, colloids from the water, particle and floc size (Lick et al.
29 1997).

how?

isn't it about the same?

31 A key process in cohesive sediment dynamics is the flocculation process, i.e. the possibility of
32 primary, individual particles to form larger aggregates or flocs, composed of many small individual

→ Not only, also the double layer interaction

1 particles. The particle yield strength determines whether colliding particles aggregate and form
2 larger flocs or disaggregate due to the collision-induced shear stress or by fluid forces, i.e. flow
3 shear. These flocculation processes significantly alter the properties of fine-grained sediments in
4 terms of the effective particle size, the particle density and the floc structure, ~~expressed by the~~
5 ~~fractal dimension~~. It is clear that the characteristics of cohesive sediments differ strongly from the
6 properties of coarser cohesionless particles. Consequently, numerical models ^{that} ~~which~~ do not include a
7 flocculation ~~algorithm~~ would make incorrect predictions when simulating small scale processes.

8 In this paper, we introduce a physics-based flocculation algorithm based on McAnally (1999),
9 which was implemented in SSIIM 3D. SSIIM 3D is a three-dimensional numerical model solving
10 the Navier-Stokes equations and the convection-diffusion equation for suspended sediment
11 transport. For the calibration and testing of the algorithm we use experimental data in annular
12 flumes (Hillebrand 2008, Klassen 2009). The aim of the simulation is to achieve a good agreement
13 between the results of the simulation and the measurements as a prerequisite for further applications
14 of the transport functions. In our simulations we model the temporal development of measured floc
15 sizes, affected by aggregation processes, as well as the measured sediment concentration. Within
16 the simulation of the settling behavior, we use different formulas for calculating the settling velocity
17 (Stokes 1850 vs. Winterwerp 1998) and include the fractal dimension to take into account the
18 structure of flocs. This paper aims to investigate the influence that the settling velocity formula and
19 the floc structure have on modelling the deposition of cohesive sediments.

↳ wasn't also flocculation?

21 **2 EXPERIMENTS IN THE ANNULAR FLUME**

22 **2.1 Experimental set-up of the annular flume**

23 Annular flumes are commonly used as a test rig for laboratory studies on cohesive sediments since
24 the flocculation processes are not interfered with by pumps and an infinite flow can be generated
25 (Haralampides et al. 2003, Hillebrand 2008, Krishnappan 2006).

26 At the Karlsruhe Institute of Technology (KIT) in Germany there are two annular flumes with a free
27 water surface which differ only in scale but not in their principle functioning. Both flumes consist
28 of a rotating inner cylinder within an outer non rotating cylinder. The rotating inner cylinder
29 generates the flow in the water column between both cylinders (see Fig. 2).

30 A major characteristic of the test rig are the distinct secondary currents due to the ~~curve~~ and the
31 rotation of the annular flume.

curvature

Not clear, can you please explain better? And also say what the

1 For all experimental and simulation results presented in this paper one setup of boundary conditions ^{boundary}
2 in the small flume was used due to a reduced computation time compared to the large flume (the ^{conditions}
3 basin diameter of the small flume is 1.20 m, the diameter of the large flume is 3.60 m. The width of ^{flume?}
4 the cross sections is 0.375 m for both flumes and the water depth was kept constant at 0.28 m).

5 2.2 Flow field measurements and simulation in SSIIM 3D

6 In previous studies the hydraulic characteristics of the two test rigs have been analyzed by three-
7 dimensional measurements using Acoustic Doppler Velocimetry and by three-dimensional
8 numerical modeling in SSIIM 3D (Hillebrand 2008, Hillebrand and Olsen 2010). Experimental data
9 on flow velocities by magnitude and flow direction as well as the turbulent kinetic energy
10 distribution were compared with the results of the simulation. Good agreement was found for both
11 the time-averaged flow field and the turbulence characteristics. Discrepancies were most significant
12 in the determination of the magnitude of the turbulent kinetic energy, but general characteristics of
13 the distribution of the TKF were the same. This is a crucial prerequisite for the further simulation of
14 flocculation processes and sedimentation of cohesive sediments in the annular flume. A detailed
15 description of the flow-field simulation in the annular flume is given by Hillebrand and Olsen
16 (2010).

Not clear...

the velocities?

what is it? Define.

This sounds like a contradiction

17 2.3 Experimental method and techniques

18 In both annular flumes several experiments by Hillebrand and Klassen were carried out. For the
19 calibration of the implemented flocculation algorithm, measured laboratory data from one
20 experiment in the small flume were used (Klassen 2009). In the experiment, the temporal
21 development of floc sizes, affected by aggregation processes, as well as the suspended sediment
22 concentration were measured at one point in the middle of the height of the water level (= 0.14 m)
23 and in the middle of the flume width. The experiment was carried out in tap water. In order to
24 simplify the complex system of natural sediments, which contain significant amounts of clay
25 minerals as well as a certain range of organic material (Raudkivi 1998), industrially processed
26 Kaolinit was used. Kaolinit is a typical representative for clay minerals and is part of the mineral
27 class of the layer silicates. In our experimental studies, the used Kaolinit had a medium grain
28 diameter of $D_g = 2.06 \mu\text{m}$.

why only one if there were many experiments?

Turbidity and concentration are not the same thing!!

29 For measuring the suspended sediment concentration the turbidity was recorded continuously
30 (every 30 seconds) combined with taking sediment samples. In order to verify aggregation
31 processes floc sizes were measured simultaneously using the In-Line microscope Aello 7000. All

X

X

1 measurements were conducted at one point in the middle of the flume width. Figure 3 shows the
2 arrangement of the measuring devices in the small flume.

3 The floc size measuring system Aello consists of a 38 mm wide stainless-steel pipe with a 8 mm
4 wide slot acting as the measuring volume (see Fig. 4). On the one side of the slot the illumination
5 devices is placed which provides the backlighting for the pictures. On the other side of the slot a
6 microscope objective and a CCD-camera with a resolution of 1024 x 768 pixels are positioned. At
7 the end of the stainless-steel pipe a box for camera electronics and electronic connections is located.
8 An image recognition software analyzes the pictures and calculates characteristic parameters for
9 particle size distributions, like the median diameter d_{50} , the particle diameter d_{16} , d_{84} or the Sauter
10 diameter. In this paper, we use the mean diameter d_{50} as a representative parameter for
11 characterizing the particle size distribution, which is based on the diameter of approximately 1000
12 measured particles. *→ What are the algorithms to calculate the diameter?*

13 Prior to the start of the experiment, a dry amount of sediment was weighed to achieve an initial
14 concentration of $C_0 = 500$ mg/l. After adding tap water, the sediment-water-suspension was mixed
15 intensively by using a laboratory stirrer. A high stirrer frequency was used to break up possible
16 flocs due to mixing. Before adding the sediment suspension in the annular flume, tap water was
17 filled inside the flume to a height of 0.28 m. The sediment suspension was then added near the inner
18 rotating cylinder to achieve a fast mixing of the suspension due to the high flow velocities and
19 turbulence intensity at the rotating wall. The rotational frequency of the inner cylinder was set to 22
20 rpm (revolutions per minute). This frequency results in a horizontal velocity of approx. 0.2 m/s near
21 the rotating boundary, decreasing to a horizontal velocity of nearly zero near the outer non rotating
22 wall. At the beginning of the measurements a high frequency of samples was necessary due to the
23 rapid turbidity decrease. In the further experiment the sampling was based on the degree of the
24 turbidity decrease. Concurrently, particle sizes were measured with an interval of 15 minutes.

I think that is the turbidity

25 **2.4 Experimental results**

26 In Fig. 5 and 6 the measured data from the selected experiment in the small annular flume are
27 shown. Figure 5 illustrates the measured total suspended sediment concentration presented over a
28 time of nearly 5 hours. In Fig. 6 the corresponding measured median diameter d_{50} and the d_{90} of the
29 particles / flocs of Kaolinit can be seen over a time of 5 hours with an interval of 15 minutes. It
30 should be taken into account, that in fact, the experiment took about 70 hours until only approx. 7
31 per cent of the initial sediment material was in suspension, i.e. almost the whole sediment mass

*ok, why not showing all 70 hours?
5*

1 determines the floc density, the particle yield strength and the collision-induced shear stresses *refer to*
2 which in turn influence the settling velocity and the aggregation mechanism. In previous sensitivity *earlier*
3 analyses, realized by adopting a simple test case in a stagnant water column in SSIIM 3D, the *experm.*
4 aggregation processes to variations in fractal dimensions were studied (Klassen et al. 2011). It could
5 be shown that the fractal dimension has a major impact on the overall mass settling. Thus, the
6 fractal dimension should be taken into account for modeling the experiments in a physically correct
7 way. In the next chapter, first the main concept of fractal theory of floc structure is presented
8 shortly and the applied values for the fractal dimension for the numerical simulation are given.

or estimated?

9 3.1 Fractal theory of floc structure and application to the numerical model

10 The main concept of fractal theory is the self-similarity of the floc structure, i.e. the fact that a
11 growing entity shows the same structure as at its initial state (Mandelbrot 1982). Therefore, growing
12 fractals are treated as scale-invariant objects (Vicsek 1992). Real fractal structures are an
13 idealization, since every geometrical body has a smallest and largest dimension (Khelifa and Hill
14 2006, Nagel 2011). In spite of this limitation several models use the approach of fractal structures in
15 order to characterize the properties of flocs. *Not clear what you mean ...*

16 The floc structure (expressed by the fractal dimension n_f) has an impact on the floc density, the
17 particle yield strength and the collision-induced shear stresses. The floc density in turn influences
18 the settling velocity, thus the deposition of fine particles. The particle yield strength in connection
19 with the collision-induced shear stresses determine if two colliding particles aggregate or
20 disaggregate due to the collision-induced shear stresses, meaning that the fractal dimension
21 influences the aggregation mechanism as well. *Collision breaks up is not likely because drag would prevent it*

22 The fractal dimension decreases from the value $n_f = 3.0$ for small and compact particles with particle
23 sizes close to the primary particles to about $n_f = 1.0$ for large and irregular flocs with an open and
24 porous structure, as indicated in Fig. 10. For example, if the flocs are connected on one line, the
25 fractal dimension is about 1, while if they are on a flat plane, the dimension is 2. And a snowflake
26 with equal distribution in all three spatial directions would be a value of about 3.

27 The smaller the fractal dimension is, the smaller is the floc density, the particle strength and the
28 collision-induced stresses. Applying the fractal theory to a settling velocity formula is the main
29 difference compared to Stokes' settling relation (1850), which treats particles as solid Euclidean
30 spheres with $n_f = 3.0$.

1 Numerical models, including the fractal dimension, often consider an overall constant value for n_f
2 for the whole floc size spectrum (Kranenburg, 1999; Xu et al., 2008). These models often assume
3 an average value for the fractal dimension such as $n_f = 2.0$.

4 However, several previous studies proposed the concept of a variable fractal dimension since they
5 showed improvements in predicting the floc size distribution and the floc settling velocity (Khelifa
6 and Hill, 2006; Maggi, 2007; Son and Hsu, 2008). The suggestion of including a variable fractal
7 dimension is based on the idea that there is a transition during the growth from the smaller
8 Euclidean, primary particles to larger real fractal aggregates. This leads to a decrease of the fractal
9 dimensions as floc sizes are increasing (Maggi, 2007). According to this theory, primary particles
10 should have a value of $n_f = 3.0$, whereas large flocs should have fractal dimensions of about $n_f = 2.0$
11 and smaller. Once the flocs have reached a certain size, they can be treated as real fractals. The
12 value of their fractal dimension is constant and depends only on the flow conditions or the particle
13 concentration. Two ranges of behavior were observed in regards to the fractal dimension of flocs at
14 a constant turbulent shear rate by Kumar et al. (2010). In the first region, for floc sizes less than 200
15 μm , a variable fractal dimension was needed to describe the submerged specific gravity as a
16 function of floc size. In the second region, for floc sizes greater than 200 μm , a constant fractal
17 dimension was found to suffice in describing the submerged specific gravity. The constant fractal
18 dimension for this second region was $n_f = 2.3$ for fresh water flocs and $n_f = 1.95$ for salt water flocs
19 (Kumar et al. 2010).

20 In this paper we used the formula for the variable fractal dimension based on previous studies of
21 Khelifa and Hill (2006). They proposed a power law to describe the variable fractal dimension
22 which depends on the floc size D_j and the primary particle size D_g :

23
$$n_f = \left(\frac{D_j}{D_g} \right)^\alpha$$
 This formula was in my PhD thesis Maggi 2005 (1)

24 with $\alpha = 3$ and

25
$$\frac{\log(n_{fc} / 3)}{\log(D_{fc} / D_g)}$$
 (2)

26 where n_{fc} represents a characteristic fractal dimension and D_{fc} a characteristic floc size. Khelifa and
27 Hill recommend the typical value for n_{fc} and D_{fc} to be $n_{fc} = 2.0$ and $D_{fc} = 2000 \mu\text{m}$, if they are not
28 measured or calculated. However, they also showed that the predicted effective density is very
29 sensitive to the parameter n_{fc} . The magnitude of the fractal dimension depends on the mechanism by
30 which aggregates grow. Flocs formed by particle-cluster aggregation have fractal dimensions

value (not magnitude)

1 higher than those formed by cluster–cluster aggregation, even if they are of the same size. Thus, in
 2 case of uncertainty regarding the characteristic values, the range of n_{fc} has to be considered in
 3 models describing flocculation processes. In this study, several values for the characteristic fractal
 4 dimension n_{fc} were applied to take into account the effect of variations of n_{fc} on the aggregation
 5 processes: $n_{fc} = 1.4, 1.7, 2.0, 2.3$ and 2.6 . According to the measured mean particle diameters d_{50}
 6 shown in Fig. 6, we set the value for the characteristic floc size D_{fc} randomly to $15 \mu\text{m}$.

7 Figure 11 illustrates the impact of the value of the characteristic fractal dimension n_{fc} on the range
 8 of the effective fractal dimension n_f . Adopting n_{fc} to 1.4 yields a size dependent fractal dimension in
 9 the range between $n_f = 3.0$ for the primary particles of size $2.06 \mu\text{m}$ to n_f of about 1.0 for larger
 10 flocs in the range of $30 - 50 \mu\text{m}$ (blue curve). In contrast, applying $n_{fc} = 2.6$ results in much more
 11 compact aggregates, since the fractal dimension for a particle size spectrum between $2.06 \mu\text{m} - 50$
 12 μm is between 3.0 and 2.4 (red line). These significant differences in floc structure due to various
 13 fractal dimensions are indicated qualitatively by the pictures of the flocs, showing rather fragile
 14 flocs for $n_{fc} = 1.4$ and more dense aggregates for $n_{fc} = 2.6$.

15 3.2 Settling velocity formula

16 As shown in the previous chapter, fractal flocs can be characterized by their floc size, their structure
 17 and their density. These properties in turn are influenced by the flow conditions (turbulence) or by
 18 the sediment characteristics, like the sediment concentration or the cohesion of the particles.
 19 Accordingly, the settling velocity of flocs can be calculated depending on many factors.

20 In order to take into account that aggregates are fractal entities, we use the settling velocity formula
 21 based on Winterwerp (1998). In this equation the floc structure is accounted for by using the fractal
 22 dimension to compute the effective density $\Delta\rho_j$ of each particle size class D_j . The effective density
 23 $\Delta\rho_j$ results from the difference between the density of each particle size class, ρ_j and the fluid density
 24 $\rho_w = 1000 \text{ kg/m}^3$. The density of each particle size class, ρ_j , is determined by the following equation
 25 (McAnally and Mehta, 2000):

26

$$27 \quad \rho_j = \text{smaller of} \left\{ \begin{array}{l} \rho_w \\ B \left(\frac{D_g}{D_j} \right)^{3 n_f} \end{array} \right. \quad (3)$$

1 where ρ_g = grain density of primary particles (set to 2650 kg/m³); ρ_w = fluid density (= 1000 kg/m³);
 2 B_p = an empirical sediment- and flow-dependent density function. For sediment in still water B_p
 3 becomes to 1650 kg/m³; D_g = primary grain diameter and n_f = fractal dimension (= 1.0 to 3.0).

4 Hence, by deriving a balance of forces between the drag force and the lift force, the settling velocity
 5 formula $W_{S,j}$ by Winterwerp (1998) in still water becomes:

6 $W_{S,j}(\text{Winterwerp}) = \frac{D_j^2}{18} g \frac{\alpha \beta}{w} \quad \rightarrow \text{this is the same as Stokes with a coefficient in front. Would it be more valuable to review more recent developments of}$ (4)

7 where α, β = particle shape coefficients. For spherical ($\alpha = \beta = 1$), solid Euclidean particles, i.e. $n_f =$ the
 8 3.0, the equation reduces to a standard Stokes settling relation, which does not consider the fractal ^{settling}
 9 dimension (Stokes, 1850): velocity?

10 $W_{S,j}(\text{Stokes}) = \frac{D_j^2}{18} g \frac{\alpha \beta}{w} \quad \leftarrow \text{Also, what have you used for } \alpha \text{ and } \beta? \quad (5)$

11 We compare the results using the implemented flocculation algorithm in combination with the
 12 settling velocity by Winterwerp (1998) with the results obtained by excluding flocculation
 13 processes and using Stokes' (1850) settling velocity which does not consider the fractal structure.

14 The simulation results in terms of applying various characteristic fractal dimensions n_{fc} and using
 15 the settling velocity formula based on Winterwerp are presented in the next chapter. Afterwards, the
 16 results by neglecting the flocculation processes of cohesive sediments and adopting Stokes settling
 17 velocity are illustrated.

19 **4 Simulation results and discussion**

20 **4.1 Number of size classes and initial conditions**

21 Modeling flocculation and fragmentation processes requires the definition of a discrete number of
 22 size classes and the corresponding particle sizes. In this study a size class-based model (SCB) was
 23 used to describe the particle size spectrum (Maerz et al., 2011, Verney et al., 2011). The SCB model
 24 is based on the population equation system that describes the floc population in N discrete size
 25 classes. Each of the used N discrete size classes corresponds to a specific particle size D_j and a
 26 related particle mass M_j , where the particle mass of each size class is determined from the density,
 27 assuming that all particles are spherical (McAnally, 1999):

28 $M_j = \frac{D_j^3}{6} \rho_g \quad \rightarrow \text{So, are they fractal? They can be fractal and spherical, but then the parameters } \alpha \text{ and } \beta \text{ in Winterwerp are 1, so, you should get the Stokes velocity again}$ (6)

1 The density ρ_j in turn is calculated depending on the fractal dimension (see eq. 3). Each particle
 2 mass, M_j , is represented by a mass class interval, which contains particles with the smallest particle
 3 mass $M_{j(lower)}$ and the largest particle mass $M_{j(upper)}$ of this class. Based on a linear mean
 4 formulation of M_j , the mass class interval is calculated by (McAnally, 1999):

$$5 \quad M_{j(upper)} = \frac{M_j + M_{j-1}}{2} \text{ with } M_{j(upper)} = M_{j-1(lower)} \quad (7)$$

6 The particle sizes are logarithmically distributed starting from the smallest primary particle
 7 diameter D_g to the maximum floc size D_{max} by using the following equation (Maerz et al. (2011)):

$$8 \quad D_j = D_g^{1 + (i-1)/(N-1) (\log_{10}(D_{max})/\log_{10}(D_g) - 1)} \quad (8)$$

9 In this study $N = 10$ size classes were defined. According to the size of the primary particles of
 10 **Kaolinit** in the experiment the minimum diameter was set to $D_g = 2.06 \mu\text{m}$. The maximum floc size
 11 was defined based on the measured floc sizes, captured by Aello. In Fig. 12 all measured flocs sizes
 12 within the first 5 hours of the experiment are shown.

13 Most particles were found in the range between 4 and 10 μm . Due to the limitations of the image
 14 recognition software, the smallest particle sizes were detected to about 4 μm (it should be noted that
 15 probably smaller particles were in suspension which could not be detected by the software),
 16 however the largest flocs have a size in the range between 30 - 50 μm . Hence, the coarsest particle
 17 size class was set to $D_{max} = 35 \mu\text{m}$, which is related to a specific particle mass, thus to a mass class
 18 interval. The largest particle mass $M_{j(upper)}$ of this class corresponds to the maximum measured floc
 19 size of 50 μm . In table 1 the chosen particle size classes ($N = 10$) for the numerical model in SSIIM
 20 3D are listed, as well as the initial concentration C_0 in each size class, which was defined randomly
 21 to achieve an initial total concentration of $C_0 = 500 \text{ mg/l}$. A different choice of initial concentrations
 22 C_0 in the size classes would result in a different initial floc size. However, Son and Hsu (2008), for
 23 example, observed that the initial floc size affects only the time to reach the equilibrium state, but
 24 not the final (equilibrium) floc size. Son and Hsu (2008) have shown, that their model results are
 25 insensitive to this uncertainty as far as the final floc size is concerned.

26 **4.2 Simulated concentrations and median floc diameters due to variations in** 27 **fractal dimension**

28 In Fig. 13 and Fig. 14 the results from the numerical simulations adopting different values for the
 29 characteristic fractal dimension n_{fc} ($D_{fc} = 15 \mu\text{m}$ is constant for all calculations) are shown. The
 30 settling velocity by Winterwerp was used for all analyses.

1 Figure 13 illustrates the total concentration development of the measured values (red, jagged line)
2 and the simulated curves by conducting a sensitivity analyses in terms of the characteristic fractal
3 dimension n_{fc} , resulting in various fractal dimensions n_f (cf. Fig. 11). Both the experiment and
4 simulation results, that are shown in the graph are recorded at the same point in the annular flume
5 (in the middle of one cross section, at the half of the water depth).

6 First of all it can be seen in Fig. 13 that the simulation is very sensitive to different characteristic
7 fractal dimensions. The concentrations are decreasing faster by adopting higher values of n_{fc} ,
8 resulting in higher fractal dimensions n_f . These results seem reasonable due to the fact that the floc
9 density increases with higher values of n_f (see eq. 3), causing a higher settling velocity. Higher
10 settling velocities in turn lead to a faster deposition of the sediment mass. Adopting the
11 characteristic fractal dimension to $n_{fc} = 1.4$ yields the best agreement with the measured data, since
12 the slope of the concentration curve is less steep as for the other simulations.

13 Nevertheless, the initial decrease of the concentration as it is indicated in the experiment is not
14 simulated in the same way by any of the simulation results. Here, a sensitivity analysis of the initial
15 conditions could bring an improvement. One factor resulting in a stronger decrease of the
16 concentration could be that a certain portion of the particles (the coarser ones), added initially in the
17 annular flume, do not exhibit fractal structures and settle down as near-solid Euclidean spheres with
18 $n_f \approx 3.0$, causing a faster initial decrease of the concentration. In the model this could be
19 implemented by defining size classes, that do not have fractal structures and are excluded from the
20 flocculation process. This issue should be verified for the next simulations.

21 In the case of $n_{fc} = 1.4$, the range of the fractal dimension n_f in the simulation is between 1.0 and 3.0
22 for the detected particle size spectrum. However, most of the aggregates, which are larger than 15
23 μm , would imply a fractal dimension of 1.4 and lower, meaning that these aggregates have an open
24 and fragile structure.

25 Although deviations between experiment and simulation were found in respect of the initial
26 concentration decrease, it could be shown that the simulation is very sensitive to the fractal
27 dimension and tendencies in the concentration evolution are similar by using a characteristic fractal
28 dimension of 1.4. The development of the corresponding simulated median diameters d_{50} confirms
29 that agreement is best by setting n_{fc} to 1.4 as it is shown in Fig. 14.

30 In Fig. 14, the respective calculated median diameter is presented over 5 hours. The red line
31 represents the data from the experiments, the other lines are the simulation results by using different
32 characteristic fractal dimensions. In the experimental results, the peak of the median floc diameter

have you calculated R and residuals? Or is only visual?

I believe that 5 hours is too short a comparison to say that this is a good agreement

Agreement is poor....

1 (11 μm), 17 minutes after adding the sediment suspension in the annular flume indicates
2 flocculation. Then a decrease of the median diameter follows which is probably caused by the
3 deposition of the larger particles. This increase in floc size followed by a decrease in aggregate size
4 appears for all calculation results. Thus, in general, aggregation processes are simulated for all cases
5 (sect. 4.3 shows the simulated flocculation process for $n_{fc} = 1.4$ in detail, illustrated by the shifting
6 of particle mass between the size classes).

7 In Fig. 14, the value of the characteristic fractal dimension determines the maximum floc size, the
8 time to achieve the maximum floc size and the slope following the peak. The best result is based on
9 a characteristic value $n_{fc} = 1.4$. For $n_{fc} = 1.4$, the median diameter is increasing, as aggregation
10 processes take place, to a maximum value of 9.5 μm and then is decreasing slightly. For $n_{fc} = 2.6$
11 the maximum median diameter is 18 μm . Then, the median particle size is also decreasing, but the
12 slope is much steeper compared to $n_{fc} = 1.4$. The higher maximum median diameter for $n_{fc} = 2.6$
13 can be attributed to the more flow resistant particles, resulting from higher fractal dimensions.
14 Adopting $n_{fc} = 2.6$ leads to more compact particles / flocs, which are not broken up by flow-induced
15 stresses that easily compared to weak particles with lower fractal dimensions. Large and weak flocs
16 ($n_{fc} = 1.4$) disaggregate due to flow-shear and lead to a shifting of particle mass in the smaller size
17 classes (see Sect. 4.3). In the case of $n_{fc} = 2.6$ not all flocs of the same size disaggregate due to their
18 more compact structure. Thus, the shifting in smaller size classes due to disaggregation caused by
19 flow-induced stresses, is not that significant. This results in a larger maximum median diameter.
20 The steeper slope of the d_{50} for $n_{fc} = 2.6$ is caused by the higher density of the compact particles,
21 leading to a faster decrease of these particles.

22 Differences are also found in terms of the time to achieve the maximum floc diameter. While this
23 measured median diameter is detected 17 min after adding the suspension in the flume, the
24 calculated maximum floc diameter is reached after about 1.2 hours (for $n_{fc} = 2.6$ after 1.3 hours),
25 decreasing afterwards slower than in the experiment. In spite of these deviations it can be
26 summarized that adopting a characteristic fractal dimension of $n_{fc} = 1.4$ and using the settling
27 velocity based on Winterwerp we get the best agreement with the measured data. The flocculation
28 process, which is shown in particular in the next chapter, can be simulated and gives plausible
29 results. Excluding these flocculation processes and using the settling velocity based on Stokes
30 would give poor results in comparison to the measured data (see Sect. 4.4).

what values of α and β ?

1 4.3 Simulated flocculation processes by shifting of particle mass through the size 2 classes

3 The flocculation process is realized by shifting mass through the size classes. Using the most
4 appropriate value for the characteristic fractal dimension $n_{fc} = 1.4$ ($D_{fc} = 15 \mu\text{m}$) results only in the
5 aggregation type 2A1, i.e. two colliding particles are always strong enough to resist the collision
6 induced shear stress and form larger aggregates. Disaggregation is only caused by flow-induced
7 stresses, which lead to a break-up of the weakest particles of size class 1, 2, 3 and 4 (for example,
8 adopting $n_{fc} = 2.6$ would cause disaggregation by flow-induced stresses only of size class 1). These
9 particles have a fractal dimension n_f in the range between $n_f = 1.0 - 1.5$, meaning that these
10 aggregates have a porous and fragile structure. Figure 15 shows the temporal development of the
11 concentrations of each size class. The decrease of the concentration of the smaller size classes 7, 8,
12 9 and 10 and the shifting of mass into the larger particle size classes 4, 5 and 6 illustrate the
13 aggregation of type 2A1. Size class 1 and 2 are immediately destroyed by the flow shear, resulting
14 in an abrupt decrease of the concentration in the first few seconds and in a shifting of the
15 concentration ~~in~~ ^{to} the smaller size classes. Particle size class 3 and 4 will also break up due to fluid
16 forces, but concurrently mass is shifted in these classes by the aggregation processes of the smaller
17 aggregates resulting in an increase of the concentrations. Hence, in Fig. 15 the shifting of
18 concentrations has to be interpreted as a result of flocculation processes, break-up due to fluid
19 shear, as well as simultaneously occurring deposition. These processes overlap, but dominant
20 mechanisms can be estimated over time. It can be seen that the flocculation process is most
21 significant for about the first hour of the simulation similar to the experiment. Afterwards
22 aggregation processes further occur, but the deposition of the sediment material dominates then.

→ not clear

23 4.4 Simulation results obtained by excluding flocculation processes and using the 24 settling velocity based on Stokes

25 Figure 16 and 17 show the results obtained by excluding flocculation processes and using the well-
26 known settling velocity formula based on Stokes (1850), which does not consider the fractal nature
27 of flocs. It is a commonly used method for calculating settling velocities of fine sediments in
28 numerical models which do not include a flocculation algorithm.

29 In Fig. 16, again the measured concentration (red line) as well as the simulated concentrations (blue
30 and green lines) over a time period of 5 hours are shown. The blue line represents the above
31 mentioned results using a characteristic fractal dimension of 1.4. The green line is calculated when

→ This entire section is a bit a trouble, I believe. See extended comments

1 the flocculation algorithm is not used in the numerical model and the settling velocity based on
2 Stokes is adopted, while all other settings are identical. Figure 17 illustrates the corresponding
3 median diameter d_{50} over time. It can be seen that the concentration is decreasing much faster when
4 excluding flocculation processes and using Stokes, yielding insufficient results in comparison to the
5 measured data. We get insufficient results with respect to the median diameter as well (see Fig. 17).
6 If no aggregation processes occur, the aggregates settle down as individual particles, which results
7 in a more abrupt decrease of the median diameter due to the deposition of the larger particles
8 leaving the smaller ones in suspension.

9 Although the calculated median diameter d_{50} is much smaller by using Stokes than the one based on
10 Winterwerp, the corresponding concentration is decreasing faster illustrating the impact of the floc
11 structure on the settling velocity. Using Stokes' settling velocity implies that all particles are treated
12 as solid Euclidean particles, i.e. $n_f = 3.0$, including a density of $\rho_g = 2650 \text{ kg/m}^3$. By contrast,
13 adopting Winterwerp's approach and considering the fractal dimension yields a decreased density
14 with increasing floc sizes. Thus, for the same particle size the settling velocity based on Stokes is
15 much higher than using Winterwerps' equation, as indicated in Fig. 18. In particular, these
16 differences become larger for large flocs with a porous and fragile structure represented by lower
17 fractal dimensions.

18 The significantly higher settling velocities based on Stokes are responsible for the stronger decrease
19 of the sediment mass. It can be seen, when excluding flocculation processes and using the well-
20 known Stokes' settling equation, we get insufficient results using the same initial grain size
21 distribution. A better agreement with the measured data could be achieved by lower sedimentation
22 rates. This would require even finer particles which in turn would not conform with the measured
23 data. The simulation results show that taking into account flocculation processes and using a
24 settling velocity formula which considers a reduced density yields better results than excluding
25 aggregation mechanisms. In this study, taking into account the used clay mineral Kaolinit and the
26 chosen hydraulic flow conditions, the implemented flocculation algorithm achieves the best results
27 for a characteristic fractal dimension of $n_{fc} = 1.4$ and for a characteristic floc size of $D_{fc} = 15 \text{ }\mu\text{m}$. In
28 the future work the calibration of the algorithm has to be optimized by sensitivity analyses in terms
29 of the initial conditions of the numerical calculation. Aside from the initial conditions of the
30 simulation also boundary conditions in terms of modeling simultaneously occurring erosion could
31 be checked. For the sake of simplicity the erosion process was neglected in these numerical studies.
32 For the next numerical simulations potential resuspension of deposited particles could be included.

1 The calculation of erosion would result in a slower decrease of the sediment mass which would
2 corresponds more to the measured data.

3

4 5 Conclusions and Application

*No, it was the turbidity
No, you basically used Stokes ($\alpha = \beta = 1$)*

5 In this study experimental data from studies in annular flumes (Klassen 2009, Hillebrand 2008)
6 were used to test and calibrate a flocculation algorithm in SSIIM 3D, which is based on McAnally
7 (1999). Both measured floc sizes as well as the sediment concentration of the experiment were
8 modeled over a time period of the first 5 hours of the experiment. Within the simulation, in order to
9 take into account the fractal structure of flocs, we included the fractal dimension and used the
10 settling velocity formula based on Winterwerp (1998), which accounts for a lower density with
11 increasing floc size. The fractal dimension decreases from the value $n_f = 3.0$ for small and compact
12 particles to about $n_f = 1.0$ for large and fragile flocs. In our study a variable size-dependent fractal
13 dimension was considered, expressed as a function of floc and primary particle size, and which also
14 depends on a characteristic fractal dimension n_{fc} and a characteristic floc size D_{fc} (Khelifa and Hill
15 2006). The sensitivity of the flocculation process to the parameter n_{fc} was studied by adopting
16 different values for this parameter ($n_{fc} = 1.4, 1.7, 2.0, 2.3$ and 2.6) and setting the characteristic floc
17 size D_{fc} constant to $15 \mu\text{m}$. The simulation results show that the flocculation process and the settling
18 behaviour is very sensitive to variations in the fractal dimension.

already known

19 ① The higher the fractal dimension of the particles/flocs is, i.e. the more dense and compact
20 the particles are, the faster the concentration is decreasing.

shall to be given evidence

21 ② Adopting Winterwerp's formula for the settling velocity, we get the best agreement with the
22 measured concentration for $n_{fc} = 1.4$, indicating that many flocs exhibit an open and porous
23 structure.

24 ③ The temporal evolution of the simulated median diameter d_{50} yields also the best result for
25 $n_{fc} = 1.4$.

26 However, the initial decrease of the concentration as it is indicated in the experiment could not be
27 simulated in the same way by any of the simulation results. Here, further sensitivity analyses in
28 terms of the initial and boundary conditions would bring an improvement and optimize the
29 calibration of the flocculation algorithm. It could be shown that in general the flocculation
30 algorithm gives reasonable results and flocculation processes can be modeled in a physically
31 plausible way.

*These should already be undertaken here. However other
additional aspects should be taken into account.* 17

1 The results using the settling velocity by Winterwerp (1998) and taking into account the floc
2 structure were compared with the results obtained by excluding flocculation processes and using
3 Stokes' (1850) settling velocity which does not consider the floc structure. It could be shown, that
4 we get insufficient results when neglecting flocculation processes and using Stokes while
5 accounting for both concentration and grain size evolution.

6 The next step of our study is the validation of this calculations by further annular flume
7 experiments. In this study the calibration was carried out by laboratory data in the small annular
8 flume. Further experimental data in the large annular flume provide the opportunity for model
9 validation. Finally, these results should find application in a numerical model simulating cohesive
10 processes in nature: the flocculation algorithm will be used for further applications of the transport
11 functions to the SSIIM model of reservoirs of the Upper Rhine River, Germany. In-situ
12 measurements of the floc sizes will be used as input data for the numerical model of the barrage
13 Iffezheim, as one of the reservoirs. At the Iffezheim barrage deposition of fine-grained sediments
14 and particle-bound contaminants leads to an environmental risk and involve great economic
15 concern. Sedimentation rates of about 115.000 m³ per year are leading to a high amount of material
16 that has to be dredged (Köthe et al., 2004). In the longer term, our objective is to use the
17 implemented flocculation algorithm in combination with particle-bound and solved contaminants
18 for modeling the suspended and contaminant transport for the Iffezheim reservoir.

there were several experiments
and these should be used here to
validate the model

20 Acknowledgements

21 The study is supported by the Federal Institute of Hydrology, Germany in the framework of the
22 cooperation project “ Experimental and numerical studies of the interaction between cohesive
23 sediments, particle-bound contaminants and the water flow “.

1 **References**

- 2 Brunke, M. (1999): Colmation and depth filtration within streambeds: Retention of particles in
3 hyporheic interstices, *Int. Rev. Hydrobiol.*, 84(2), 99–117.
- 4 Haralampides, K., McCorquodale, J. A., Krishnappan, B. G. (2003): Deposition Properties of Fine
5 Sediment. In: *Journal of Hydraulic Engineering* 129, Nr. 3, p. 230–234.
- 6 Hillebrand, G. (2008): Transportverhalten kohäsiver Sedimente in turbulenten Strömungen –
7 Untersuchungen im offenen Kreisgerinne. PhD thesis, Universität Karlsruhe (TH), Germany.
- 8 Hillebrand, G. and Olsen, N.R.B. (2010): Hydraulic Characteristics of the Open Annular Flume -
9 Experiment and Numerical Modeling. The first European Congress of the IAHR. 4th-6th May 2010,
10 Edinburgh.
- 11 Hillebrand, G., Klassen, I., Olsen, N.R., Vollmer, S. (2012): Modelling fractionated sediment
12 transport and deposition in the Iffezheim reservoir. 10th International Conference on
13 Hydroinformatics, Hamburg, Germany.
- 14 Khelifa, A. and Hill, P. S. (2006): Models for effective density and settling velocity of flocs. *Journal*
15 *of Hydraulic Research*, Vol. 44, No. 3, pp. 390–401.
- 16 Klassen, I. (2009): Absinkverhalten kohäsiver Sedimente in turbulenten Strömungen – Ermittlung
17 von Skalierungseffekten der Versuchseinrichtung Kreisgerinne. Diplomathesis, Universität
18 Karlsruhe (TH), Germany.
- 19 Klassen, I., Hillebrand, G., Olsen, N.R., Vollmer, S., Lehmann, B., Nestmann, F. (2011): Modeling
20 finesedimentaggregationprocessesconsideringvaryingfractaldimensions. Proceedings of the 7th
21 IAHR Symposium on River, Coastal and Estuarine Morphodynamics, 6.-8. Sept. 2011, Beijing,
22 China.
- 23 Köthe, H., Vollmer, S., Breitung, V., Bergfeld, T., Schöll, F., Krebs, F. and v. Landwüst, C. (2004):
24 Environmental aspects of the sediment transfer across the Iffezheim barrage, River Rhine,
25 Germany. Proceedings of WODCON XVII, Hamburg.
- 26 Kranenburg, C. (1999): Effects of floc strength on viscosity and deposition of cohesive sediment
27 suspensions. *Continental Shelf Research* 19, pp. 1665–1680.
- 28 Krishnappan, B. G. (2006): Cohesive sediment transport studies using a rotating circular flume. The
29 7th International Conference on Hydroscience and Engineering (ICHE-2006), Sep. 10-Sep.13,
30 Philadelphia, USA.

1 Kumar, R.G., Strom, K.B., Keyvani, A. (2010): Floc properties and settling velocity of San Jacinto
2 estuary mud under variable shear and salinity conditions. In: *Continental Shelf Research* 30 (2010)
3 2067–2081.

4 Lick, W., Chroneer, Z., Rapaka, V. (1997): Modeling the dynamics of the sorption of hydrophobic
5 organic chemicals to suspended sediments. *Water, Air and Soil Pollution*, Vol. 99, pp. 225-235.

6 Maerz, J., Verney, R., Wirtz, K., Feudel, U. (2011): Modeling Flocculation processes:
7 Intercomparison of a size class-based model and a distribution-based model. In: *Continental Shelf*
8 *Research* 31 (2011) S84-S93.

9 Maggi, F. (2007): Variable fractal dimension: A major control for floc structure and flocculation
10 kinematics of suspended cohesive sediment. *Journal of Geophysical Research*, Vol. 112.

11 Mandelbrot, B. B. (1982): *The fractal geometry of nature*. Freeman, New York.

12 McAnally, W. H. (1999): *Aggregation and deposition of fine estuarial sediment*. PhD thesis, Univ.
13 of Fla., Gainesville, Fla.

14 McAnally, William H. and Mehta, Ashish J. (2000): Aggregation rate of fine sediment. *Journal of*
15 *hydraulic engineering*, Vol. 126, No.12, pp. 883–892.

16 Mehta, A. J., McAnally, W. H. (2007): *Fine-Grained Sediment Transport*. In: Garcia, Marcelo H.:
17 *Sedimentation Engineering: Processes, Measurements, Modeling and Particle*. ASCE Manuals and
18 *Reports on Engineering Practice* No. 110. Published by American Society of Civil Engineers.

19 Nagel, M. (2001): *Zur inneren Morphogenese von Flocken mittels Clusteranalyse*. PhD thesis,
20 Technische Universität Cottbus, Germany.

21 Olsen, N. R. B. and Skoglund, M. (1994): Three-dimensional numerical modeling of water and
22 sediment flow in a sand trap, *Journal of Hydraulic Research*, Vol. 32, No. 6, pp. 833-844.

23 Olsen, N. R. B. (2011): *A three-dimensional numerical model for Simulation of Sediment*
24 *movements In water Intakes with Multiblock option. Version 1 and 2. User’s manual*. Department
25 of Hydraulic and Environmental Engineering. The Norwegian University of Science and
26 Technology, Trondheim, Norway.

27 Raudkivi, A.J. (1998): *Loose Boundary Hydraulics*, A.A. Balkema, Rotterdam, Netherlands.

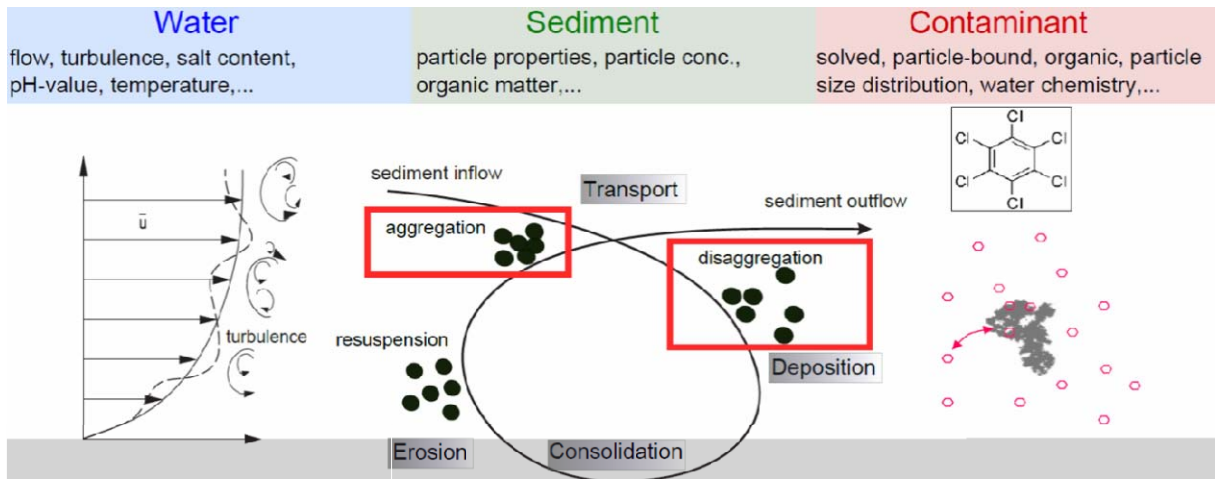
28 Son, Minwoo and Hsu, Tian-Jian (2008): Flocculation model of cohesive sediment using variable
29 fractal dimension. *Environ Fluid Mech*, 8:55–71.

- 1 Stokes, G. G. (1850). On the Effect of the Internal Friction of Fluids on the Motion of Pendulums.
2 From the Transactions of the Cambridge Philosophical Society, Vol. IX.
- 3 Verney, R., Lafite, R., Brun-Cottan, J. (2011): Behaviour of a flocculation population during a tidal cycle:
4 laboratory experiments and numerical modelling. In: Continental Shelf Research 31 (2011) S64-
5 S83.
- 6 Vicsek, T. (1992): Fractal Growth Phenomena. World scientific, Singapore.
- 7 Winterwerp, J. C. (1998): A simple model for turbulence induced flocculation of cohesive
8 sediment. Journal of hydraulic research, Vol. 36, No.3, pp. 309–326.
- 9 Winterwerp, Johann C. and Van Kesteren, Walther G. M. (2004): Introduction to the physics of
10 cohesive sediment in the marine environment. In: Developments in sedimentology, Vol. 56,
11 Elsevier, New York.
- 12 Xu, F., Wang, D.P. and Riemer, N. (2008): Modeling flocculation processes of fine-grained
13 particles using a size-resolved method: Comparison with published laboratory experiments.
14 Continental Shelf Research 28, pp. 2668–2677.
- 15 Yang, C.T. (1996): Sediment Transport: Theory and Practice. McGraw-Hill series in water
16 resources and environmental engineering.

1 Table 1. Chosen particle size classes ($N = 10$) and initial concentration C_0 for each size class for the
 2 numerical model in SSIIM 3D. Each size class is represented by a mass class interval $M_{j,upper}$ and
 3 $M_{j,lower}$.

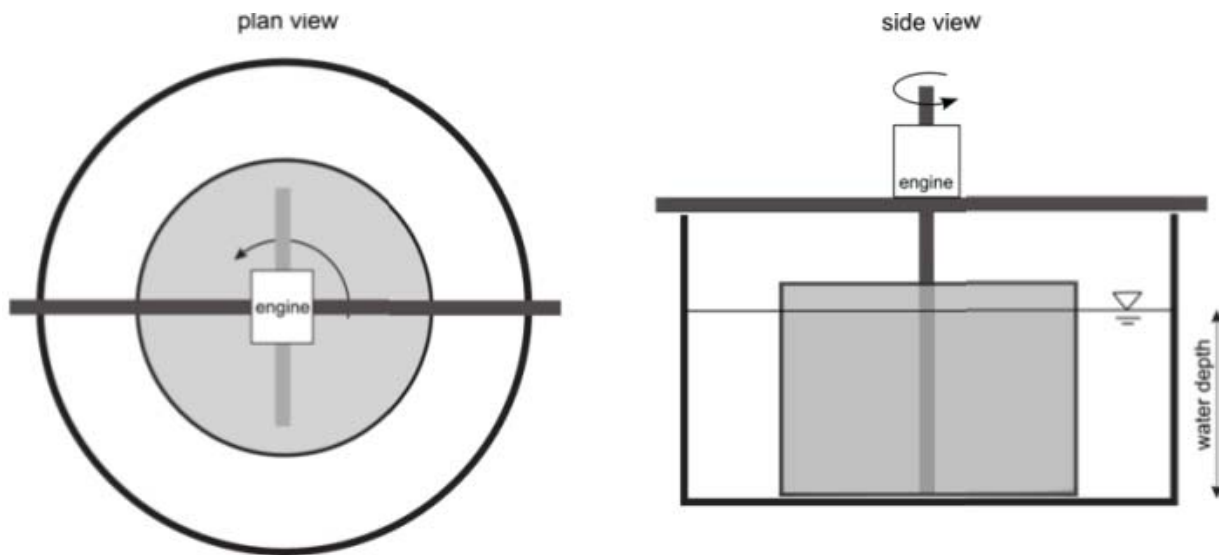
Size class	1	2	3	4	5	6	7	8	9	10
Particle size(μm)	35	25.5	18.7	13.6	9.9	7.3	5.3	3.9	2.8	2.06
C_0 (mg/l); $\sum=500$ mg/l	25	25	20	20	25	25	65	125	120	50

4

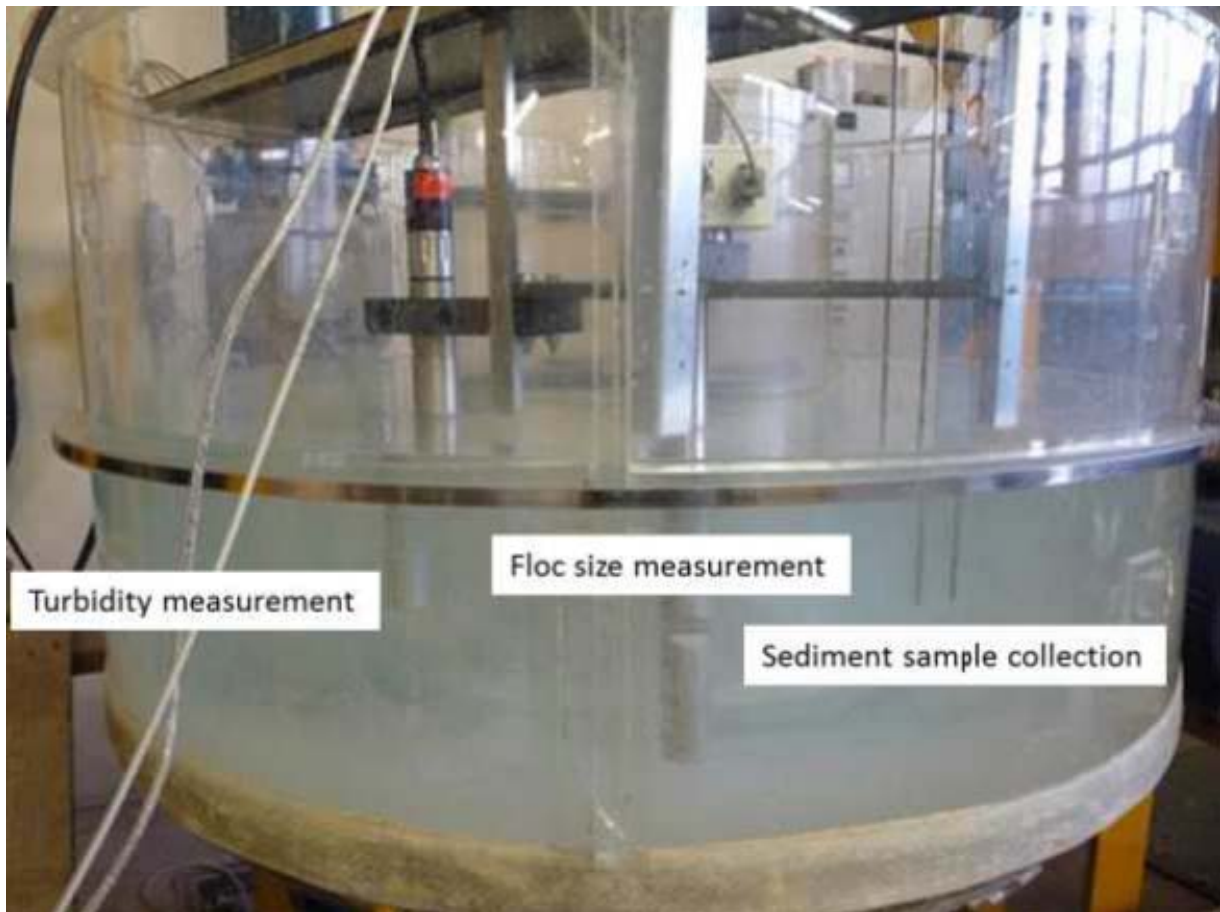


1
2

3 Figure 1: Factors influencing cohesive sediment transport.

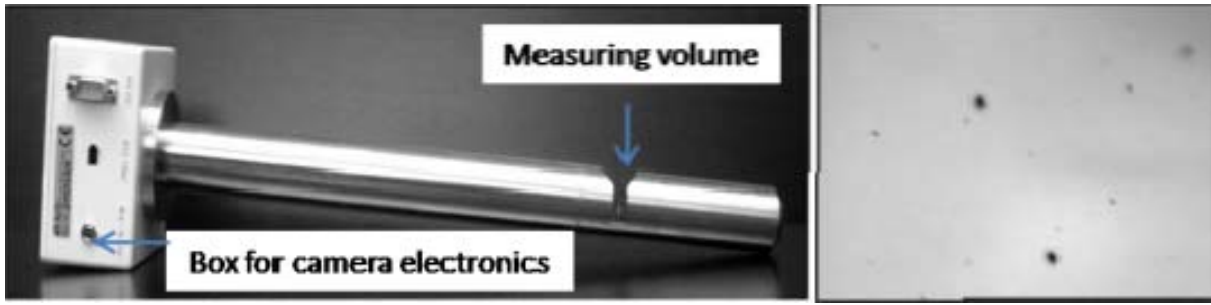


- 1
- 2
- 3 Figure 2: Simplified sketch of the open annular flume (Hillebrand and Olsen 2010).



1
2

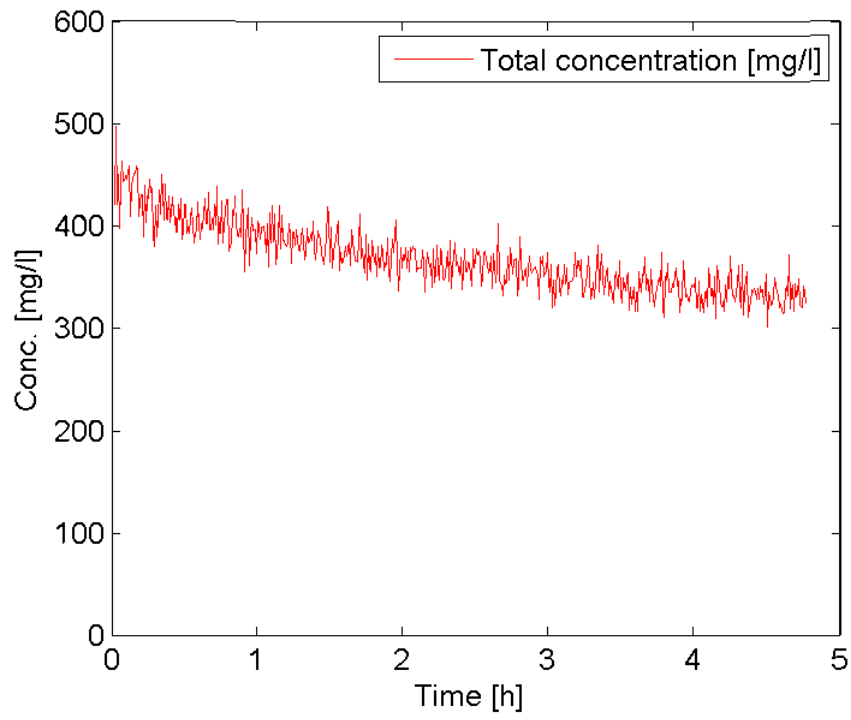
3 Figure 3: Arrangement of the measuring devices in the small flume.



1

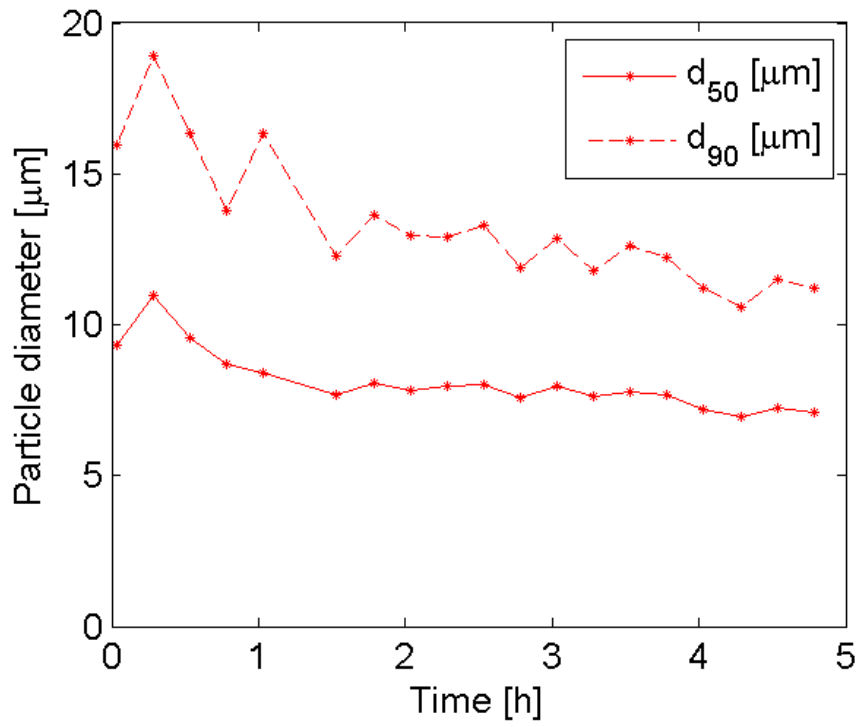
2

3 Figure 4: Aello In-Line Microscope.



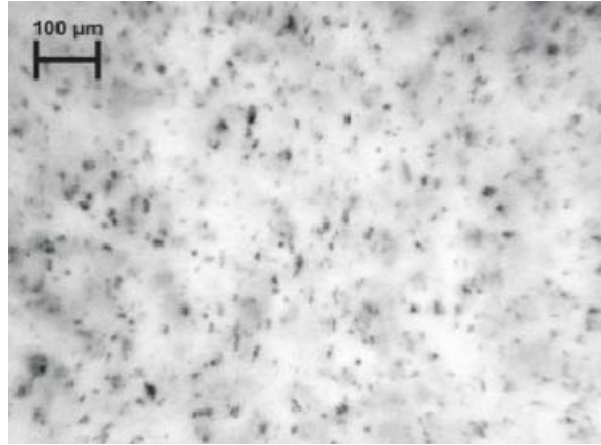
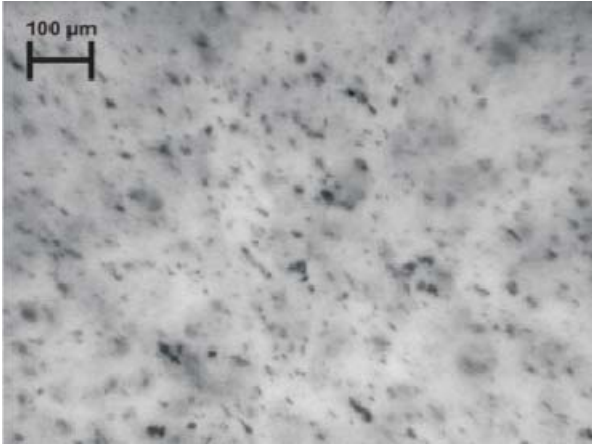
1
2

3 Figure 5: Measured suspended sediment concentration over a time of approx. 5 hours at the center
4 of the cross section.



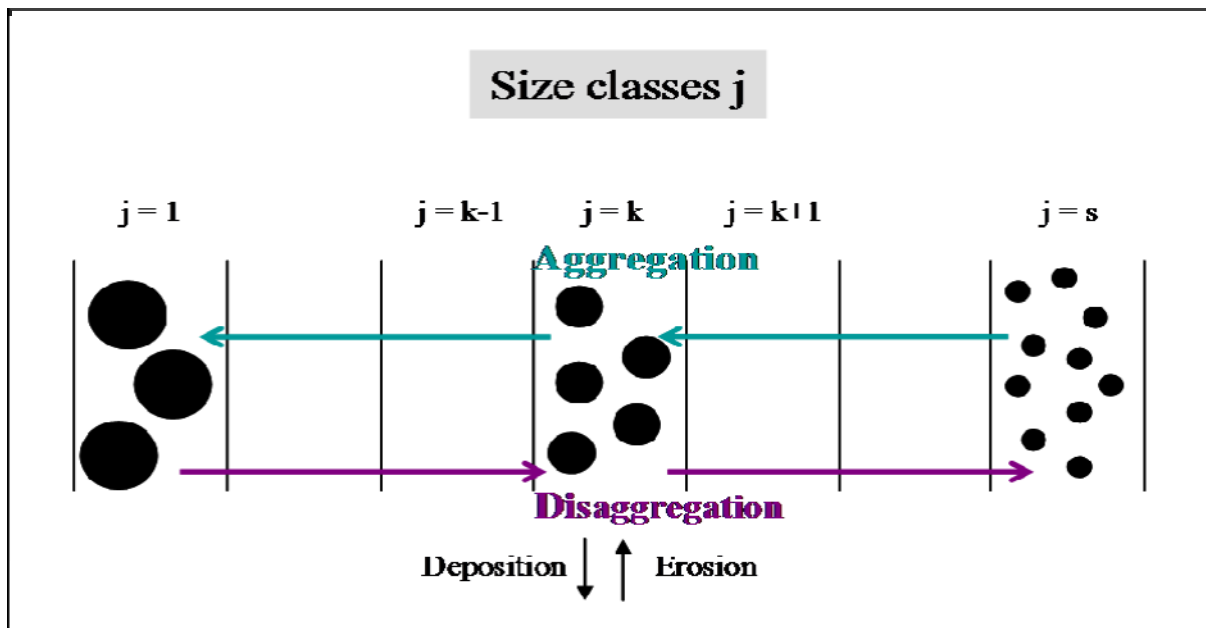
1
2

3 Figure 6: Measured median diameter d_{50} and d_{90} of the particles over a time of approx. 5 hours at
4 the center of the cross section.



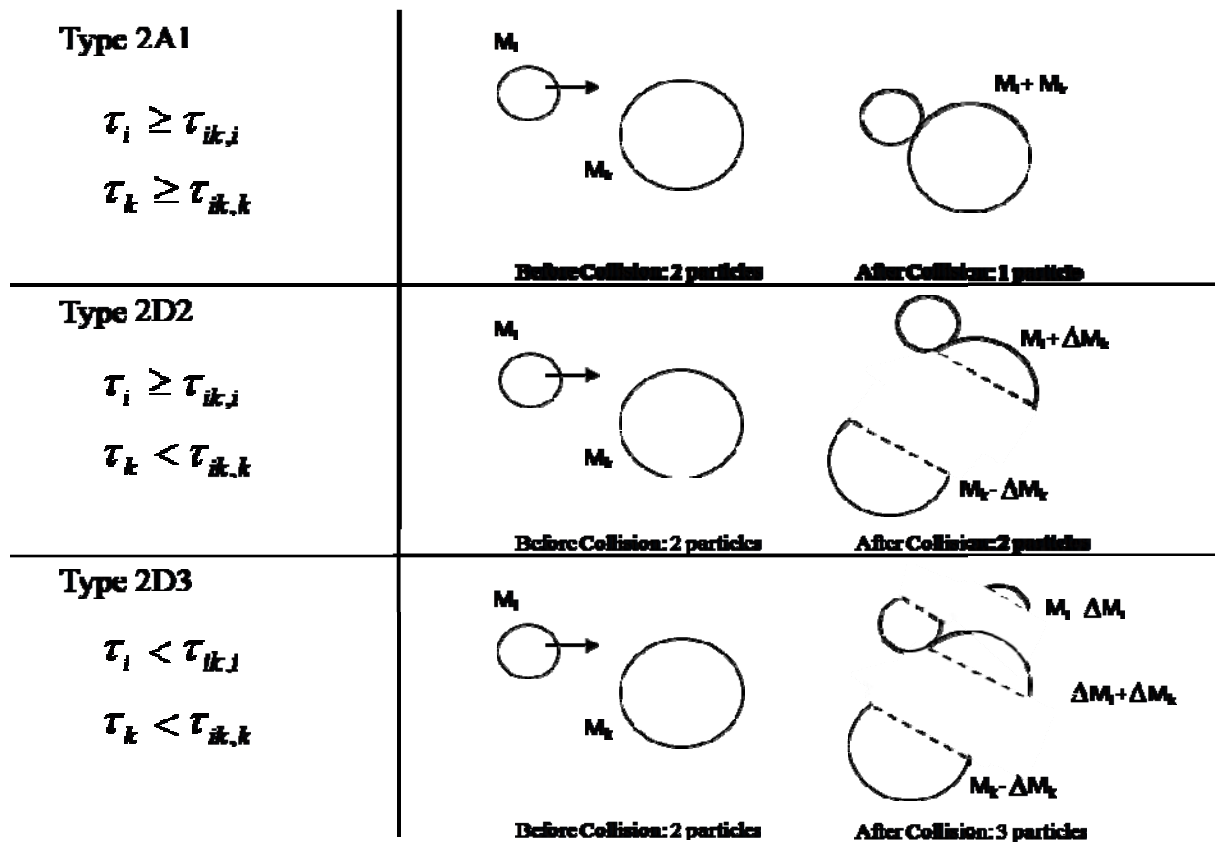
1
2
3
4
5

Figure 7: Pictures of the particles, captured by the Aello In-Line microscope (left: $d_{50} = 11 \mu\text{m}$, right: $d_{50} = 7.6 \mu\text{m}$)



1
2

3 Figure 8: Sediment mass fluxes between size classes by aggregation or disaggregation and
4 deposition / erosion (McAnally, 1999; modified)

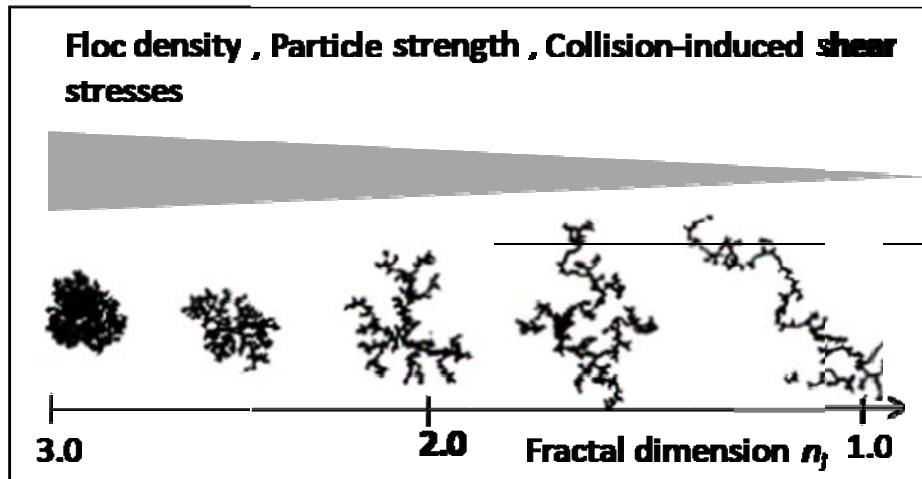


1

2

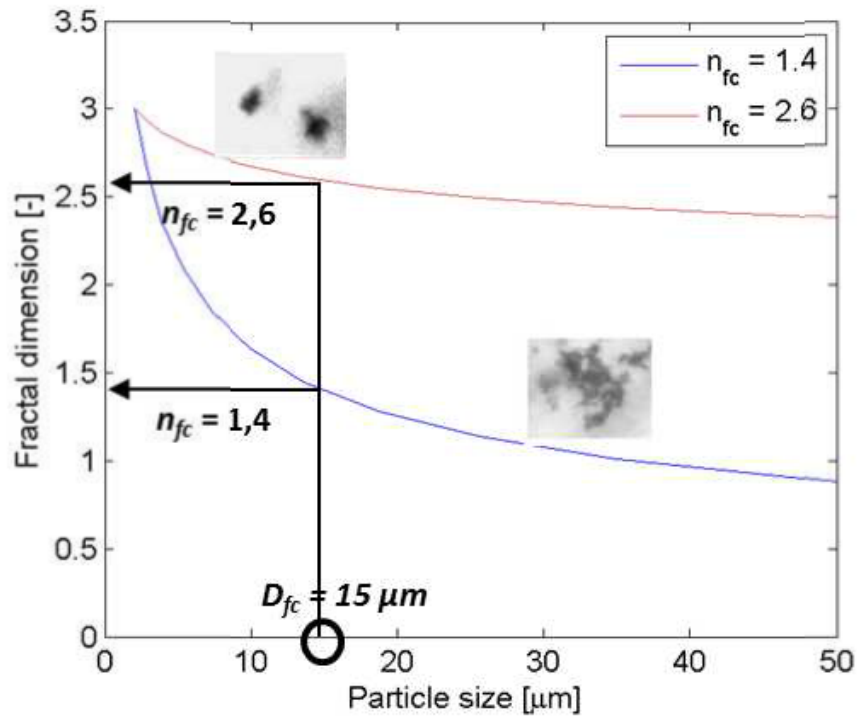
3 Figure 9: Collision outcomes depending on the strength of the particles compared with the collision

4 induced forces (McAnally, 1999; modified)



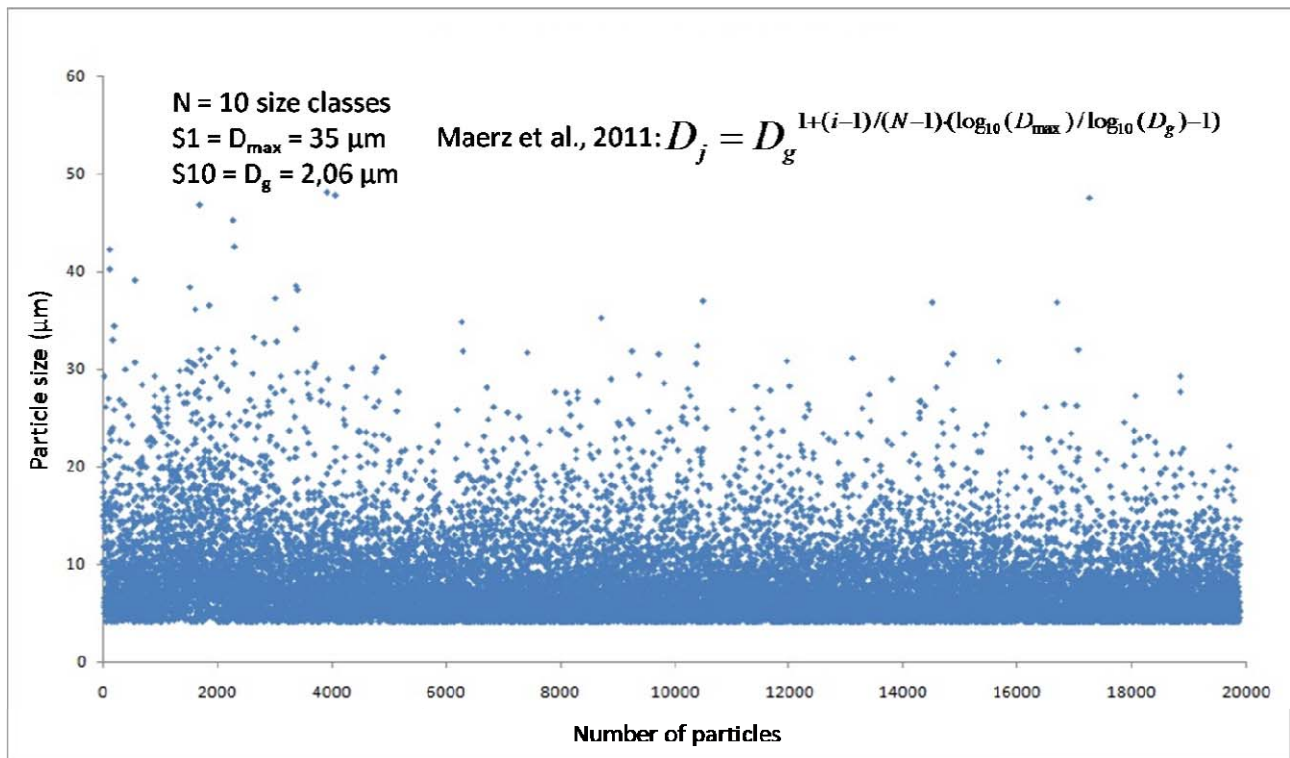
1
2

3 Figure 10: Variable fractal dimension n_f ranging from $n_f = 1.0$ for large and fragile flocs to $n_f = 3.0$
4 for small and compact particles.



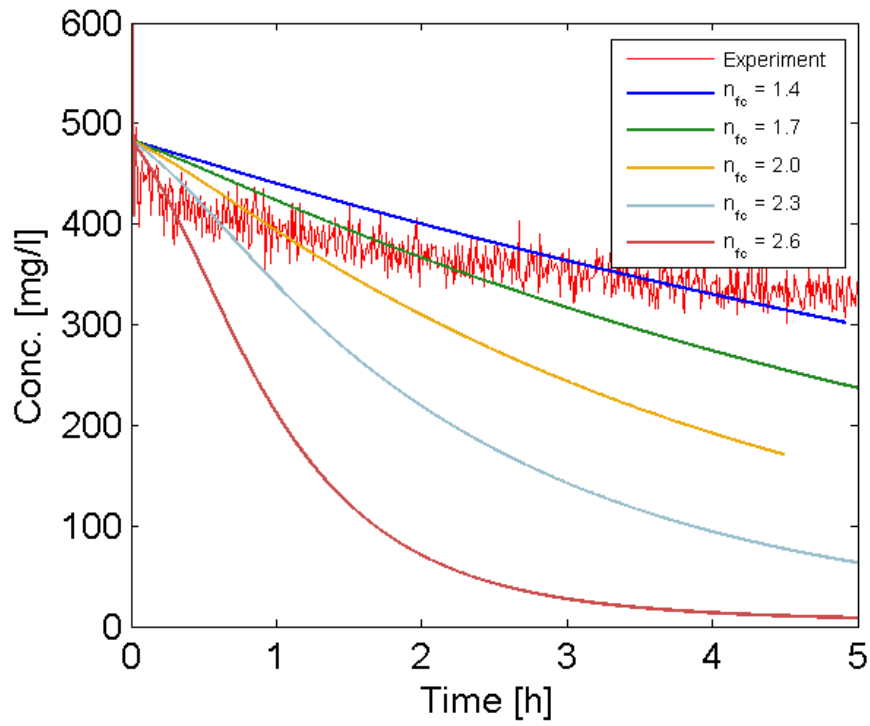
1
2

3 Figure 11: Calculated variable fractal dimension n_f depending on the characteristic floc size D_{fc} and
4 the characteristic fractal dimension n_{fc} .



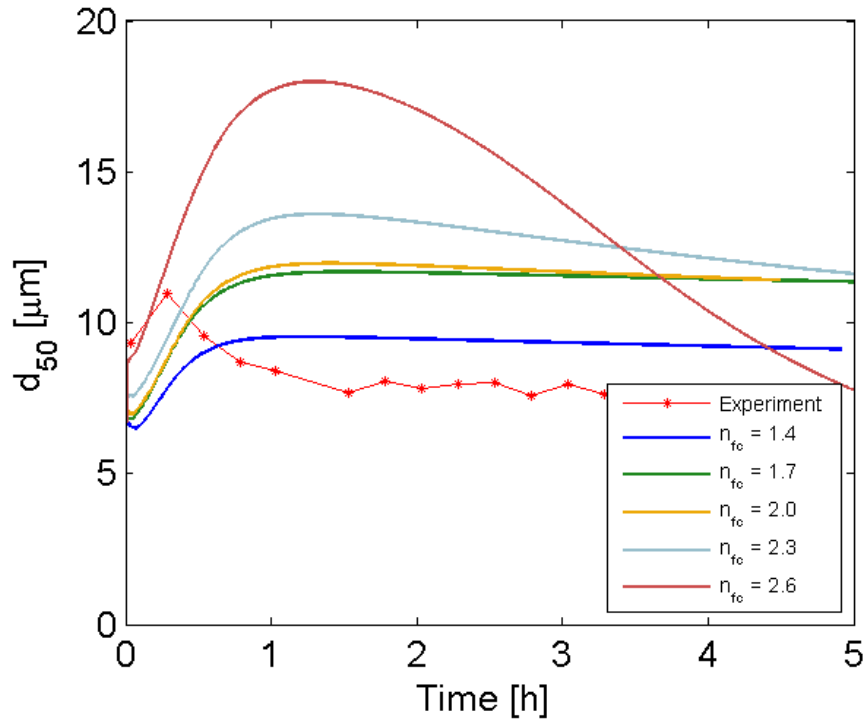
1

2 Figure 12: All measured particle sizes in the first 5 hours of the experiment.



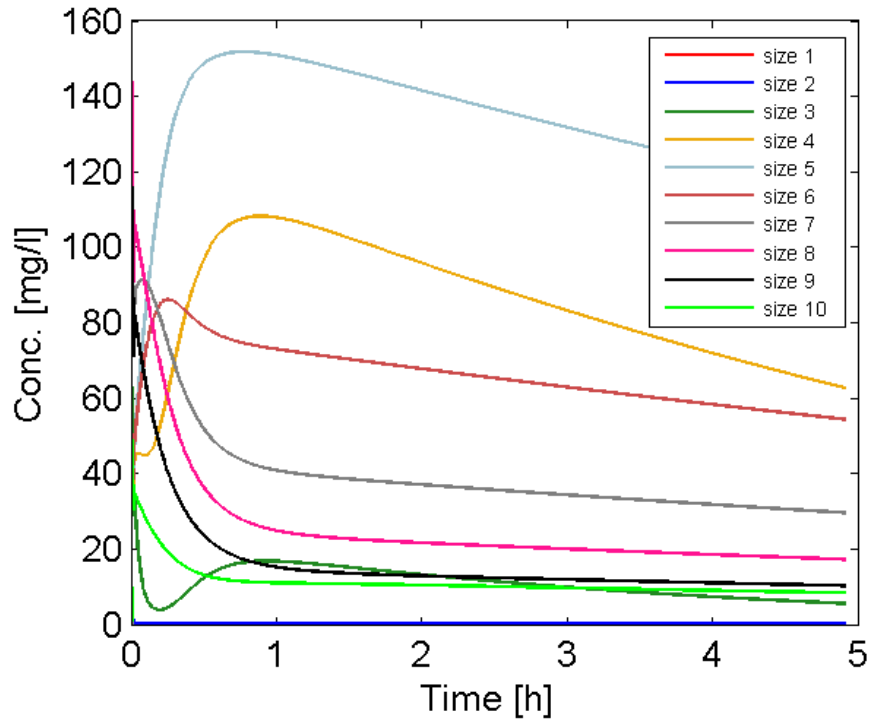
1
2

3 Figure 13: Measured concentration (red, jagged line) and calculated concentrations by using
4 different characteristic fractal dimensions n_{fc} (=1.4, 1.7, 2.0, 2.3 and 2.6).



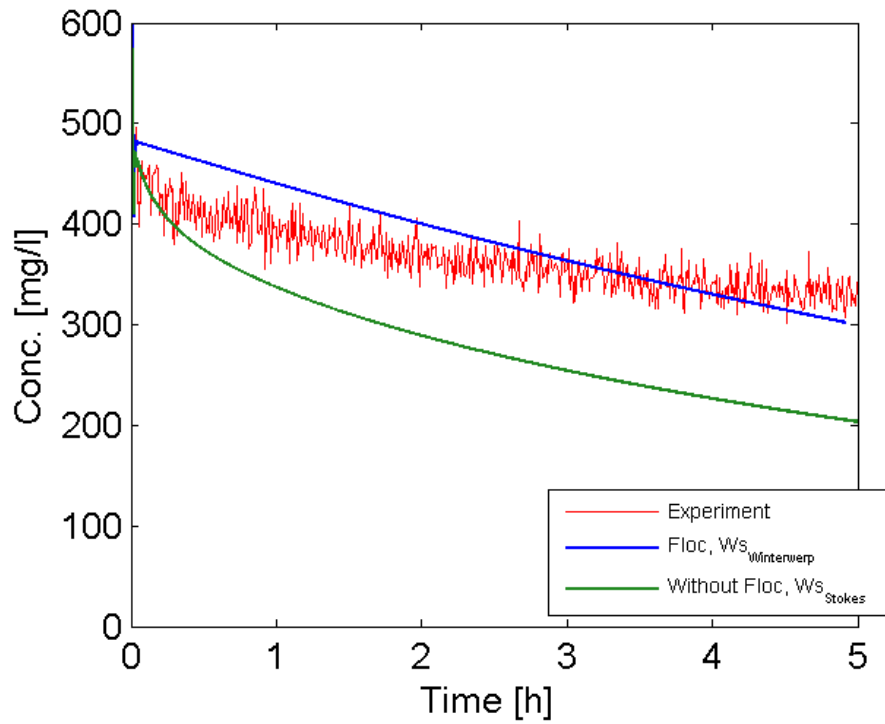
1
2
3
4
5

Figure 14: Measured median diameter (red, dashed line) and calculated median floc diameter by using different characteristic fractal dimensions n_{fc} (=1.4, 1.7, 2.0, 2.3 and 2.6).



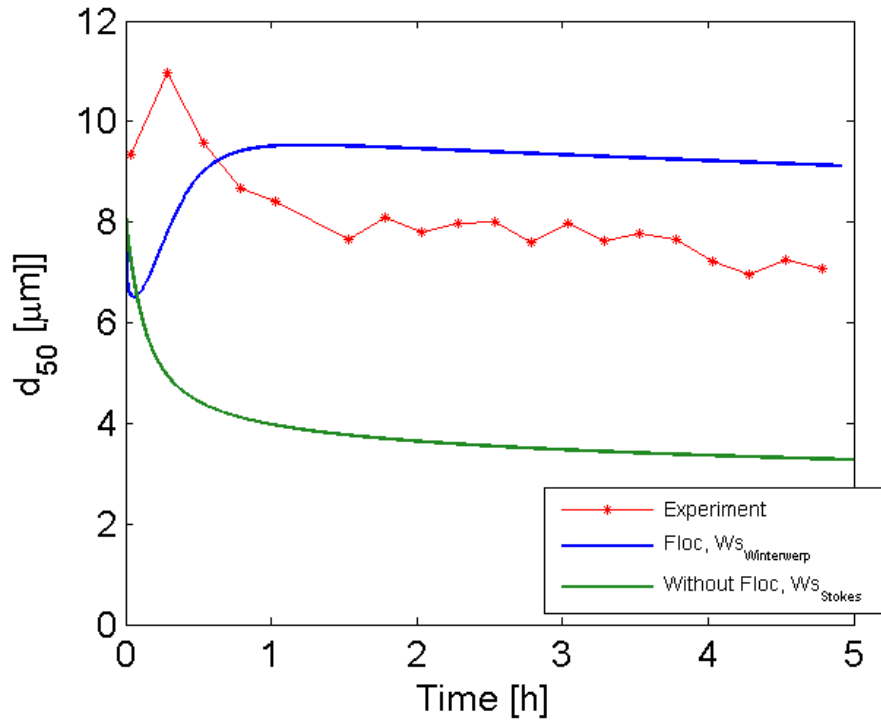
1
2

3 Figure 15: Temporal development of the concentrations of each particle size class due to
4 aggregation, break-up and deposition ($n_{fc} = 1.4$, $D_{fc} = 15 \mu\text{m}$).



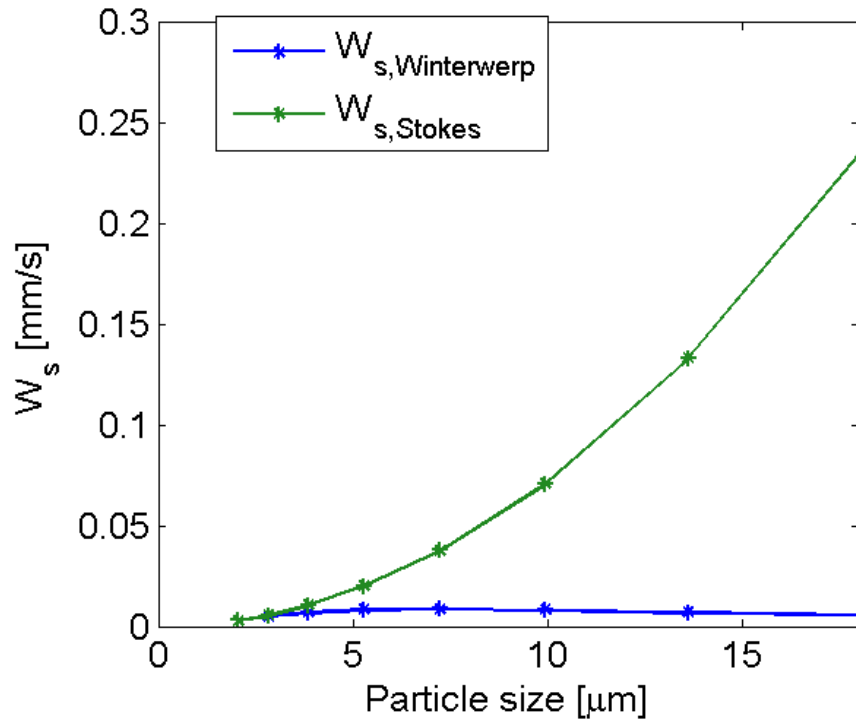
1
2

3 Figure 16: Measured concentration (= red, jagged line) and calculated concentration by using the
 4 flocculation algorithm ($n_{fc} = 1.4$, $D_{fc} = 15 \mu\text{m}$) and the settling velocity by Winterwerp (1998) (=
 5 blue line) and by excluding flocculation processes and using the settling velocity based on Stokes
 6 (1850) (= green line).



1
2

3 Figure 17: Measured median diameter (red, dashed line) and calculated median floc diameter by
 4 using the flocculation algorithm ($n_{fc} = 1.4$, $D_{fc} = 15 \mu\text{m}$) and the settling velocity by Winterwerp
 5 (1998) (= blue line) and by excluding flocculation processes and using the settling velocity based on
 6 Stokes (1850) (= green line).



1
2

3 Figure 18: Calculated settling velocity depending on the floc size by using Winterwerp's formula
4 (blue line) or Stokes equation (green line).